Spin accumulation in thin Cs salts on contact with optically polarized Cs vapor

Kiyoshi Ishikawa
Graduate School of Material Science, University of Hyogo, Ako-gun, Hyogo 678-1297, Japan
(Received 14 June 2011; published 8 September 2011)

The spin angular momentum accumulates in the Cs nuclei of salt on contact with optically pumped Cs vapor. The spin polarization in stable chloride as well as dissociative hydride indicates that nuclear dipole interaction works in spin transferring with a lesser role of atom exchange. In the solid film, not only the spin buildup but also the decay of enhanced polarization is faster than the thermal recovery rate for the bulk salt. Eliminating the signal of thick salt, we find that the nuclear spin polarization in the chloride film reaches over 100 times the thermal equilibrium.

DOI: 10.1103/PhysRevA.84.033404 PACS number(s): 32.80.Xx, 34.35.+a, 32.30.Dx, 76.60.−k

I. INTRODUCTION

Hyperpolarization, which occurs when the nuclear spin polarization is much higher than the thermal equilibrium, is one way of achieving sensitive nuclear magnetic resonance (NMR). Ionic crystals are spin polarized by paramagnetic electrons in dynamic nuclear polarization [1], and noble gases are spin polarized by optically pumped alkali-metal atoms [2]. The polarized alkali-metal atoms have also been applied to an alkali-metal salt [3]. The atoms transport the angular momentum to the salt surface, and the atomic nuclear polarization is transferred to the nuclei in the solid [4]. The Cs NMR signal was enhanced, however, only for the hydrides CsH and CsD [5]. For the first time since the demonstration of spin transfer to CsCl [4], this paper reports significant enhancement for a thin coating of the chloride on glass fibers. The spin polarization in the film builds up by optical pumping and decays in the dark. Both processes are faster than the thermal recovery in the bulk salt. Using the difference in the characteristic time, we estimate the polarization of chloride film over 100 times the thermal equilibrium. Since the chloride is thermally stable enough to remove the excess Cs metal, we can retain the surface exposed to the polarized vapor for spin transfer.

II. EXPERIMENT

The spin polarization of ^{6}Li, ^{7}Li, and ^{133}Cs nuclei decays slowly in the salt such as alkali-metal hydride and halide, due to small quadrupole moment and symmetric crystal field [6]. The salts suit for the accumulation of spin angular momentum. We use the Cs atoms to optically polarize, because the D_1 and D_2 lines are well separated in buffer gas and the applied magnetic field and because the vapor density is high enough at a moderate temperature. The quartz-glass wool has multifunctions in optical pumping, and the most important is to increase the surface area of salt exposed to polarized vapor [5]. The glass cell containing glass wool was connected to a vacuum manifold. The salt was formed on fine glass fibers in a way suitable for each salt. For the hydride, the glass wool and cell were baked at 350°C for a few days. A small amount of Cs metal was chased to the cell at room temperature, resulting in glass wool of a dark purple color. The cell was filled with hydrogen gas at atmospheric pressure and heated by torch to make the Cs metal react with hydrogen gas into a white Cs hydride. We obtained a thin film of hydride by use of this single procedure and tried several times for a sufficient amount of hydride. Finally, the cell was sealed off with Cs metal and N_2 gas at room temperature. There was a thick layer of crystallites on the sidewall of the glass cell—a major source of thermal equilibrium signals. A small amount of salt on the glass fibers should present the NMR enhancement because of the large surface area that is in contact with polarized atomic vapor.

For CsCl, the glass wool and cell were baked with grains of salt at 350°C. From the observation that the relatively cold glass wall was coated with frosty white due to sublimation of salt, we expected that the surface of glass fibers was also coated with salt film under the vapor pressure. The film was so thin that granular salt was left near the glass stem as it was before baking. The grains contribute to the thermal signal but not so much to optical enhancement. It is noted that two types of salt, film and bulk, existed together in single glass cells.

The experimental setup is shown in Fig. 1. Cs atoms were polarized by D_2 pumping for sufficiently longer than the spin relaxation time of Cs nuclei in the salts. The pump beam was linearly polarized to provide σ light for the magnetic field. Although the pump light is randomly scattered and unpolarized by the glass wool, it can polarize Cs atoms because the absorption depends on the light polarization due to the Zeeman splitting [5]. The glass cell was heated mainly by an electric heater outside the magnet, and the additional increase of approximately 5°C was indicated by laser irradiation. Because of the temperature gradient, the excess Cs metal moved away from the detection region to the stem of the glass cell. A loss of the NMR circuit reflected the distribution of metal. The vapor pressure equilibrated with the Cs metal at the coldest spot of stem. A nonmagnetic thermocouple was placed near the incidence window to measure the temperature of the salt rather than the metal. We recorded free induction decay following the excitation by a single radiofrequency (RF) pulse and summed many shots if needed. The area of the resonance peak in the Fourier transform of the transient signal gives a measure of the spin polarization enhanced by optical pumping or at the thermal equilibrium.

III. OPTICAL NMR ENHANCEMENT

The NMR enhancement in CsD has been presented in Ref. [5]. An accumulation time of 600 s was large enough to maximize the signal. The positive enhancement was 62 and

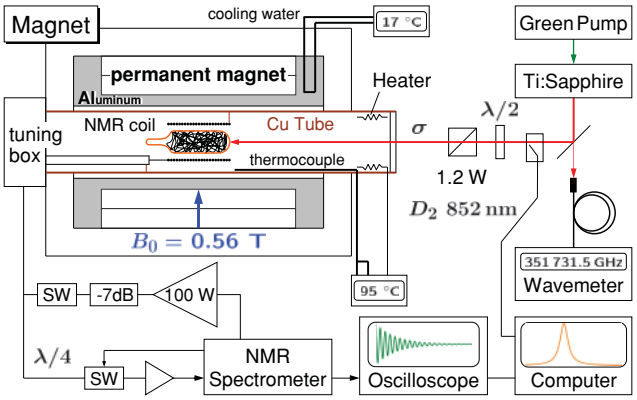

FIG. 1. (Color online) Setup for optical NMR enhancement. A salt-vapor cell was placed at 0.56 T of the permanent magnet. The field homogeneity (15 ppm) was better than the NMR linewidth of salt (300 ppm). The magnet was thermally isolated from the NMR probe with an Al block cooled by water. The NMR frequency varied due to temperature drift of magnet, but it was negligible for evaluating the spin polarization.

the negative was −80 by tuning the laser. The enhanced signals were mostly due to the thin film on the glass fibers, whereas the thermal signal also came from thick salt on the sidewall. The enhancement was tentatively obtained by comparing to this thermal signal, resulting in underestimation of the true value.

The signals for many CsCl cells were measured in a similar way to CsD. Since the spin recovery time was 590 s for bulk salt in the dark, both thermal and enhanced signals were averaged with a periodic interval 1800 s. From the thermal signal shown in Fig. 2, we expect that the cell contains a similar amount of Cs salt as the CsD cell. The enhancement is, however, an order of magnitude smaller than that for CsD. The thermal signal came from the salt on the sidewall as well as the fibers, again resulting in underestimation of enhancement. On the

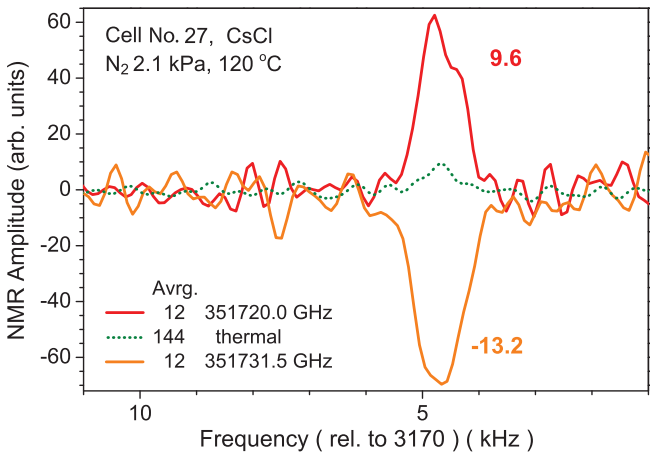

FIG. 2. (Color online) NMR signals in CsCl (28 mg) with 2.1 kPa N_2 were averaged 12 times for optical pumping and 144 times for thermal equilibrium with periodic intervals of 30 min. The enhancements were 9.6 and −13.2, respectively, at the laser frequencies 351 720.0 and 351 731.5 GHz. The linewidth is narrower than the hydrides, but a small broadening due to the drift of magnetic field was observed.

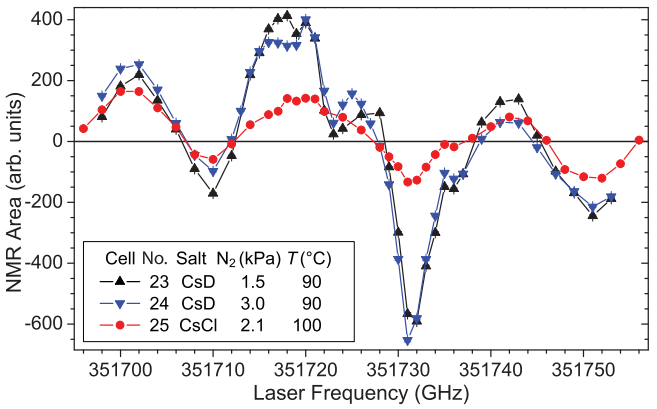

FIG. 3. (Color online) Laser-frequency dependence of the NMR area for CsD (▲, ▼) and CsCl (● first run) for the σ-polarized incident light. The signals were averaged several times with the repetition time 100 s for CsD and 200 s for CsCl.

other hand, the cell (No. 25) containing CsCl (92 mg) showed the enhanced signal that was large enough to detect by a single shot. We present three sets of measurement below the first, the second, and the third runs for this cell.

Figure 3 shows the NMR area as a function of laser frequency at the D_2 line. Because the detection was quickly repeated, the NMR area has negligible contribution of thermal signal, even for CsCl, as described below, and can be compared to the laser-induce spin current near the salt [4]. Except for the trivial difference due to the individual character of glass wool, the analogous shapes were observed for these cells. Therefore, the nuclear polarization of atoms was the primary source for enhancement in CsCl, as in the hydrides [5].

IV. SPIN-POLARIZATION RISE AND DECAY

The spin polarization was built up in CsD by use of continuous optical pumping, as shown in Fig. 4. The asymptotic value of the NMR area at a long accumulation time strongly depended on temperature, because the spin current in gas phase

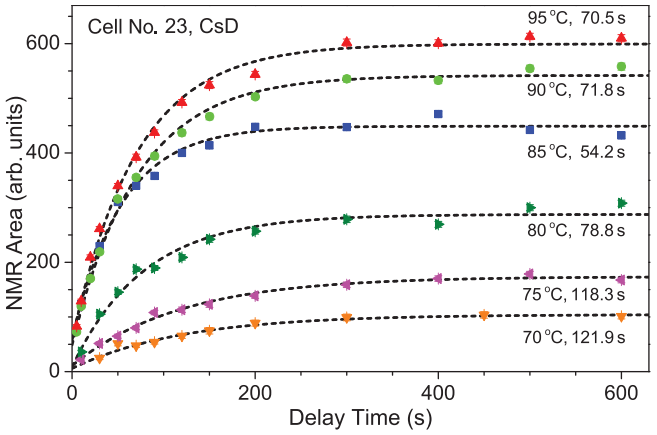

FIG. 4. (Color online) Nuclear spin polarization was positively built up in CsD by optical pumping at 351 720 GHz. Horizontal axis is the delay time of RF $\pi/2$ pulse from saturation RF pulses. The buildup time at each temperature is indicated along with a single exponential curve best fitted free at the origin ($t = 0$).

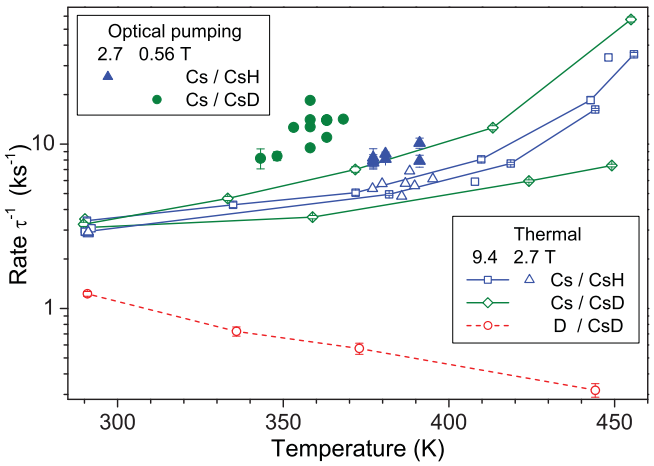

FIG. 5. (Color online) Thermal recovery rate for Cs nuclei in the hydrides (□, △, ◊) increases more rapidly than exponential without optical pumping, though the rate for deuteron (○) decreases by heating. The spin buildup rates by pumping (▲ 2.7 T, ● 0.56 T) became larger than the corresponding rates in the dark.

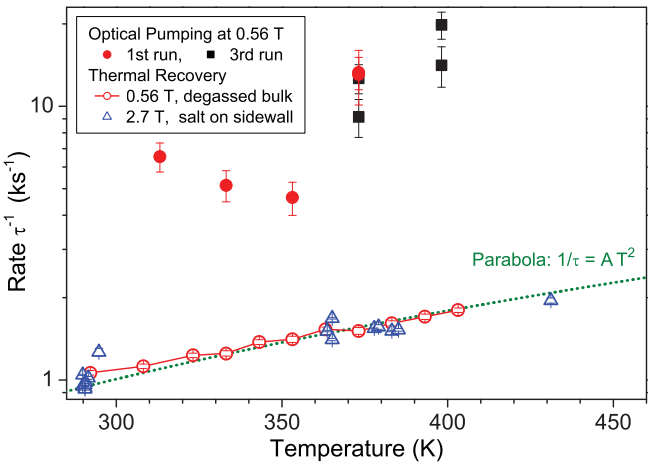

FIG. 6. (Color online) Buildup rate in CsCl for optical pumping at 0.56 T (first ●, third ■). The bulk degassed polycrystal was used as reference at 0.56 T (○), and thick salt on the sidewall of pumping cell at 2.7 T (△).

is proportional to the number density of polarized Cs atoms. The buildup rate also increased slightly by heating, as shown in Fig. 5. Since only a little hydride was available by the chemical reaction, it was difficult to measure the thermal recovery rate at 0.56 T in the dark. Alternatively, we study the recovery rate at the high fields to compare with the buildup rate by optical pumping.

Since the hydride decomposes at high temperature, the stoichiometric reaction $2Cs + H_2 \leftrightharpoons 2CsH$ is equilibrated with a few Torr of hydrogen gas at 200°C in a glass cell [7,8]. The excess Cs metal shifts the equilibrium to the right-hand side of reaction. There should be vacancies in the crystal at the temperature for optical pumping. The mass difference is so large that hydrogen ions can hop in the crystal but Cs ions stay at the stable position [9,10]. The mechanisms of spin relaxation differ for these nuclei as expected from other crystals [11,12], since the D NMR line was narrowed more than the Cs line by heating, and since the spin recovery rates exhibit the opposite temperature dependence as shown in Fig. 5. Because of the great change of crystal structure, the rate for Cs nuclei increased more rapidly than exponential. The difference between CsH (□) and CsD (◊) was less than the characteristics of glass cells. Therefore, rather than the magnetic dipole interaction with anions, the electric quadrupole relaxation is dominant in the crystal. Because of no significant difference between the Cs recovery rates at 2.7 T (△) and 9.4 T (□), the spin relaxation is mostly due to Raman process in phonon scattering [6] and we expect that the thermal recovery rate at 0.56 T is similar to that at the high fields. The buildup rates by pumping (●, ▲) were significantly larger than the recovery rate in the dark. The difference was small at 2.7 T but reliable, because the rates (▲, △) were measured for the identical glass cells with thick salt on the sidewall but *no* glass wool.

A large amount of CsCl salt was used as a reference to measure the thermal recovery rate at 0.56 T. A commercial salt was melted, degassed in vacuum, and quickly cooled down for polycrystal. The measured rate was independent of applied magnetic field, as shown in Fig. 6. At the temperatures much lower than the melting point, the linewidth was almost constant and the recovery rate depended in a parabolic way on temperature, as expected from Raman process in phonon scattering [6]. Since the dependence is more moderate than the superexponential change for hydrides, the chloride can accumulate the spin polarization even at high temperature.

As shown in Fig. 7, the spin buildup by optical pumping was faster than the spin recovery in the dark. Since the thermal signal was not fully recovered at a small delay time, the ratio of the optically enhanced signal to the thermally recovered signal increases when averaging faster. Therefore, in spite of thick salt on the sidewall, the thermal signal was negligible in the NMR area measured every 200 s, as shown in Fig. 3.

A simple model for spin polarization in a salt film, provided in the appendix, describes that the spin angular momentum is transferred from polarized vapor at the surface and diffuses into the salt by the nuclear dipole interaction. The spin polarization reaches a plateau faster than bulk salt, because the polarization leaks through the other surface if the film is thinner than the spin diffusion length. In the thin limit, the

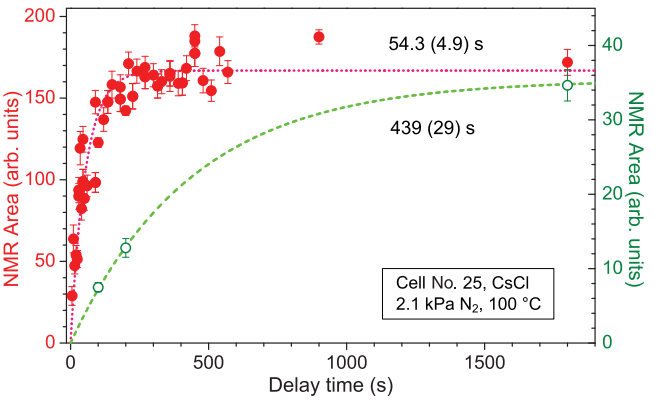

FIG. 7. (Color online) The spin buildup for CsCl in the first run by optical pumping at 351 720 GHz (● the left vertical axis) and the thermal recovery (○ the right axis). Dotted curves are the best fit by a single exponential function fixed at the origin.

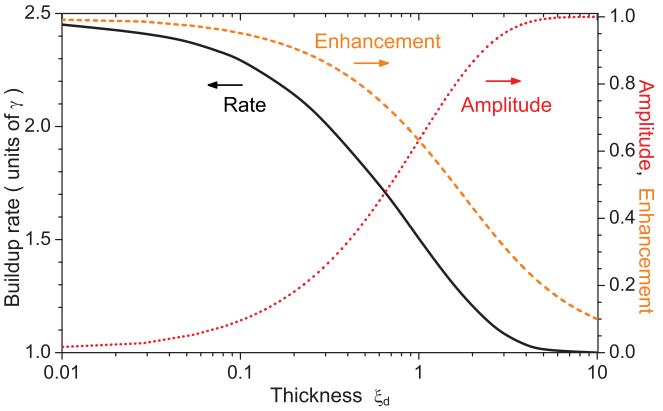

FIG. 8. (Color online) Buildup rate (black curve) at the rising edge, signal amplitude (dotted red), and enhancement (dashed orange) for $t \to \infty$ are calculated from Eq. (A3). The buildup rate is scaled by the units of γ at the left vertical axis. The amplitude is normalized by $J_s A/\gamma$, and the enhancement is by $J_s/\gamma N I_0 \lambda_d$. The thickness $\xi_d = 0.01$ corresponds to a few atomic layers since the spin diffusion length $\lesssim 100$ nm.

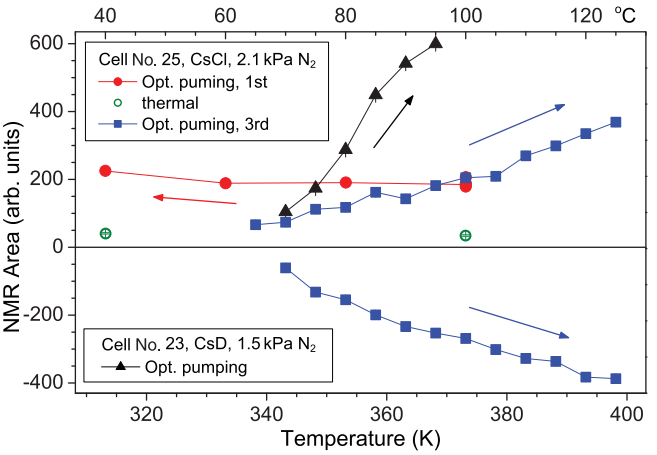

FIG. 10. (Color online) Temperature dependence of the NMR area for CsD (▲ from Fig. 4) and CsCl (● first run, ■ third run). The arrows indicate the time sequence of measurements. Negative areas are also plotted for the third run. For a wide range of temperatures, the thermal signal helps calibrate the sensitivity.

rate is enhanced by $m = 2.47$ from the intrinsic decay rate γ (see Fig. 8). Using the buildup time in Fig. 7, we estimate the recovery time for film, $1/\gamma \lesssim 54.3\, m = 134$ s, smaller than the observed time constant in the dark. Therefore, the salt exhibiting enhancement differs from thick salt producing a thermal signal on the sidewall. The spin polarization can recover fast in the film if the crystal structure differs from the bulk lattice and if paramagnetic sites are significantly produced. A method to introduce color centers is to heat the salt together with excess alkali metal. This is just happening in the pumping cells, although the color centers diffuse effectively at the higher temperature. Figure 9 shows the decay of enhanced polarization in the dark. The decay rate was nearly equal to the buildup rate but larger than the thermal recovery rate in the bulk salt. The rate for film salt was not switched whether the pump light was turned on or off.

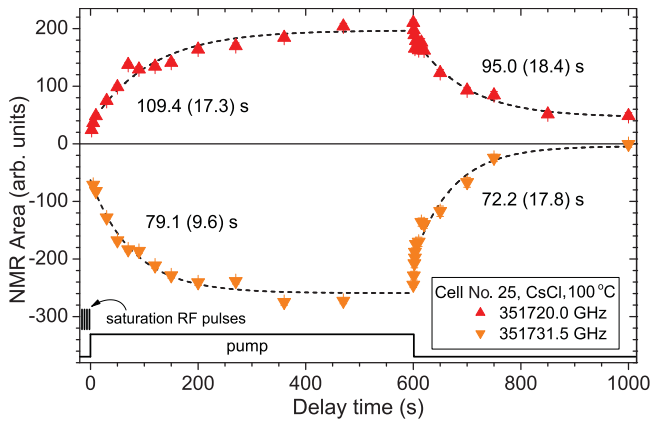

FIG. 9. (Color online) Spin rise and decay for CsCl in the third run. The inset shows the saturation RF pulses and the duration of optical pumping. A large fitting error in parenthesis means that the rising and falling edges were too fast to be described by a single exponential function (dotted curve).

V. CURING OF ALKALI-METAL SALT CELL

We have manufactured a large number of alkali-metal salt cells with an impression that functions for NMR enhancement were lost by overheating even the appearance was the same [4]. One way of finding out how to regenerate and cure the salt cells is to expose them to the cycles of heating and cooling. The chloride is suitable for the temperature cycle because of stable in optical pumping and flame heating. On the other hand, the decomposition of hydride induces the spatial redistribution of salt and would make it difficult to interpret the results.

The signal for CsD was hardly detected below 70°C. Figure 10 shows contrasting characteristics—the signal for CsCl was significantly enhanced at 40°C and stably and continuously detected by pumping for many hours after the previous acquisition at 60°C. The result means that the atom density was considerable at 40°C and the pump light should have desorbed Cs atoms from salt surface and glass fibers. The chloride cell was never heated additionally after the flame sealing, and we call this measurement the first run.

After the first run, the chloride cell was heated homogeneously at 150°C for 2 weeks. It was long enough for the Cs metal, previously placed in the glass stem, to be distributed uniformly over a whole glass cell. Since the salt on the sidewall was immersed in the Cs metal, the salt film must have been covered by the metal. In spite of the temperature gradient, we found from the quality factor of NMR circuit that much Cs metal remained in the cell body. For the second run, little enhancement was observed at each temperature. The metal, though necessary for vapor density, causes the side effect for spin transfer.

The Cs metal was removed from the salt surface by flame heating. Because of low N_2 pressure, the metal moved into the glass stem without reaction to glass. On the way, bulk salt on the sidewall presented as blue, but it disappeared within tenths of minutes. We did not find the coloration of salt on the glass wool. The salt of pure white was ready for the third run of the NMR measurement. The quality of tuning circuit was high

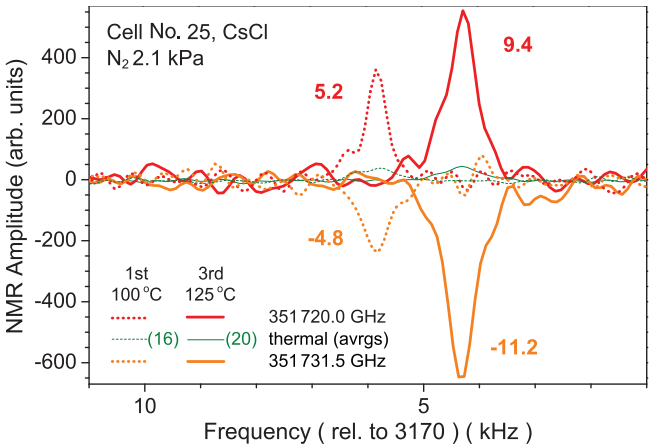

FIG. 11. (Color online) Single-shot detection of NMR signal in CsCl. The enhancement in the third run at 125°C was larger than in the first run at 100°C. Thermal signals were averaged many times. Frequency shift was due to the change of applied magnetic field according to the cell temperature.

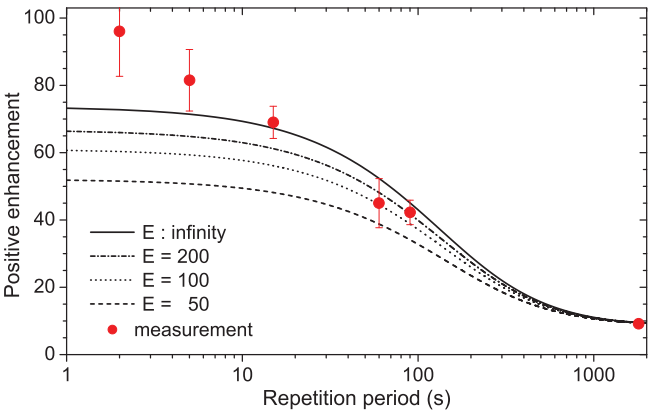

FIG. 12. (Color online) Positive enhancement (•) was measured at 125°C for the cured CsCl cell. The curves are E_R calculated for the true enhancement $E = 50$, 100, 200, and ∞ by use of $E\delta = 9.4$ in Eq. (1).

as if it was an empty cell. Once the metal was removed, the salt surface remained uncovered because of the temperature gradient. Figure 10 shows the enhancement (■) matching to temperature dependence of vapor pressure. The optimum temperature is higher than 125°C, the upper limit of the current equipment. By removing the metal thoroughly from the salt surface, we were able to regenerate the intentionally degraded CsCl cells. For the hydride, we used a torch for chemical reaction, resulting in the uncovered surface for the first run.

With the cured CsCl cell, the signal was significantly enhanced as shown in Fig. 11. We estimate the true enhancement E in the film by eliminating the thermal signal of thick salt. When the film and the thick salt have, respectively, decay rates γ_F and γ_B, the enhancement depends on the repetition period T_R as

$$E_R = \frac{\delta(1 - e^{-m\gamma_F T_R})}{\delta(1 - e^{-\gamma_F T_R}) + (1 - \delta)(1 - e^{-\gamma_B T_R})} E, \qquad (1)$$

where δ is the molar ratio of salt in the film, $m\gamma_F = 70.8\ \mathrm{s}^{-1}$ and $\gamma_B = 571\ \mathrm{s}^{-1}$, using the film model at 125°C in Fig. 6, and $E\delta \approx E_R = 9.4$ at $T_R = 1800$ s, as shown in Fig. 12. Though $E_R \approx E\delta m\gamma_F/[\delta\gamma_F + (1 - \delta)\gamma_B] \leqslant E\delta m\gamma_F/\gamma_B \approx 73$ for the fast averaging, the measured enhancement is away from the curves at $T_R < (m\gamma_F)^{-1}$ because the spin polarization built up faster at the rising edge. Since the measured enhancements were above the curve of $E = 100$ for $T_R \gtrsim (m\gamma_F)^{-1}$, the enhancement in the film was over 100, which means $\delta \lesssim 0.1$. It agrees with the insight that most of thermal signal was from thick salt. We expect the same scenario for CsD because the buildup rate was larger than the thermal recovery rate and the thick salt remained on the sidewall—the true enhancement was larger than the observed one and exceeded 100.

VI. SUMMARY

The Cs NMR signal of hydride and chloride was sufficiently enhanced by optical pumping of Cs vapor. Because of the large surface area by using glass fibers, the salt was efficiently contacted with the polarized vapor. The nuclear spin polarization in CsCl was primarily due to the atomic Cs nuclei, as in the hydrides. The thermal recovery rate in bulk salt was independent of magnetic field but depended on temperature in different ways: The chloride showed the parabolic dependence due to Raman process in phonon scattering and the hydrides presented the change of crystal structure. The optically enhanced signal rose and decayed faster than the recovery time. Eliminating the thermal signal of thick salt, we found that the enhancement in the film salt exceeded 100. We became able to cure the alkali-metal salt-vapor cells by removing alkali metal from the salt surface.

ACKNOWLEDGMENTS

The author acknowledged W. Happer, Y.-Y. Jau, B. Patton, and B. A. Olsen for comments on the experiment. The measurement at 2.7 T and 9.4 T was done by the author at Princeton University. This work was supported by the Grant-in-Aid for Scientific Research of JSPS, Japan.

APPENDIX: SPIN BUILDUP IN A THIN FILM

The angular momentum transferred from polarized atoms diffuses into a salt film. Since the spin diffusion is due to the nuclear dipole interaction in alkali-metal salt [6], the diffusion length is less than the diameter of glass fiber and the salt can be considered as a flat film of thickness d. We approximate that the diffusion coefficient D and the spin decay rate γ are isotropic and homogeneous. As shown in Fig. 13, the surface at $x = 0$ is in contact with the polarized Cs vapor, and spin current density J_a flows from the gas phase to the salt. The spin current is partly injected to the solid, where the conversion efficiency J_s/J_a ($\ll$1) should be related with D and γ since the spin transfer is mostly due to the nuclear dipole interaction. We temporarily assume that the efficiency is independent of the spin polarization at the surface and the direction of surface to magnetic field. The other surface contacts with a glass substrate at $x = d$, with the boundary condition that the spin current transmits to the substrate. The longitudinal component of nuclear spin $I(x,t) = \langle I_z\rangle(x,t)$ follows the diffusion

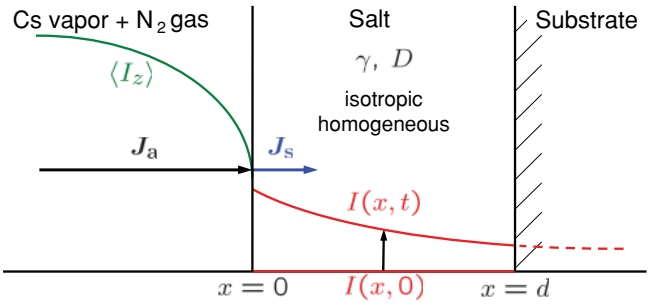

FIG. 13. (Color online) Spin transfer from polarized atomic vapor to a salt film. The initial condition $I(x,0) = 0$ is due to saturation RF pulses, and the diffusion spin current transmits to the substrate at $x = d$. J_a and J_s are the spin current density at $x = 0$, respectively, in the vapor and in the salt.

equation,

$$\frac{\partial}{\partial t}I(x,t) = D\frac{\partial^2}{\partial x^2}I(x,t) - \gamma[I(x,t) - I_0] + s(x,t), \quad \text{(A1)}$$

where $s(x,t) = (J_s/N)\delta(x)$ is the continuous source of angular momentum to the $+x$ direction at the surface, N is the number density of Cs nuclei in the salt, and I_0 is the thermal equilibrium value. We have the following solution with the initial condition $I(x,0) = 0$,

$$I(\xi,t) = I_0(1 - e^{-\gamma t}) + \frac{J_s}{N\sqrt{D\gamma}} \times \left[e^{-\xi} - \frac{2e^{-\gamma t}}{\pi}\int_0^\infty \frac{e^{-\gamma t\kappa^2}\cos(\kappa\xi)}{\kappa^2+1}d\kappa\right], \quad \text{(A2)}$$

where the distance $\xi = x/\lambda_d$ and the spin diffusion length $\lambda_d = \sqrt{D/\gamma}$. The first line on the right-hand side shows the saturation recovery to the thermal equilibrium, with no contribution to the nuclear spin current, $J(x,t) = -ND\partial I(x,t)/\partial x$, in the salt. The second term on the second line changes from $-e^{-\xi}$ to 0 for $t = 0 \to \infty$.

The amplitude of free induction decay is proportional to the magnetization and the volume of salt. We define the signal amplitude by the dimensionless quantity,

$$S = NA\int_0^d I(x,t)dx = NI_0Ad(1 - e^{-\gamma t}) + \frac{J_sA}{\gamma}\left[(1 - e^{-\xi_d}) - \frac{2e^{-\gamma t}}{\pi}\int_0^\infty \frac{e^{-\gamma t\kappa^2}}{\kappa^2+1}\frac{\sin\xi_d\kappa}{\kappa}d\kappa\right], \quad \text{(A3)}$$

where the normalized thickness $\xi_d = d/\lambda_d$ and A is the surface area. The amplitude is calculated for the cases, $\xi_d \gg 1$, $\xi_d \approx 1$, and $\xi_d \ll 1$ below.

For thick salt ($\xi_d \gg 1$), the amplitude is independent of D as follows,

$$S = A\left(NI_0d + \frac{J_s}{\gamma}\right)(1 - e^{-\gamma t}). \quad \text{(A4)}$$

Since the thermal and enhanced signals rise by the same rate γ, the enhancement $J_s/(\gamma NI_0d)$ is constant. The enhanced signal for $t \to \infty$ is equal to the injected angular momentum for the decay time $1/\gamma$. For the thickness nearly equal to the spin diffusion length ($\xi_d \approx 1$), the enhanced amplitude is $(AJ_s/\gamma)(1 - e^{-\xi_d})$. The buildup rate is numerically calculated at the rising edge $t \lesssim d^2/D$. For thin film ($\xi_d \ll 1$),

$$S = ANI_0d(1 - e^{-\gamma t}) + \xi_d\frac{AJ_s}{\gamma}[1 - \mathrm{erfc}(\sqrt{\gamma t})], \quad \text{(A5)}$$

where the error function $\mathrm{erfc}(x) = (2/\sqrt{\pi})\int_x^\infty e^{-t^2}dt$. Figure 8 shows the numerical calculation of the buildup rate, the amplitude of enhanced NMR signal, and the enhancement. Since the time profile depends on the film thickness, we evaluated the buildup rate by the inverse of time when the signal increases by $(1 - 1/e)$ to the maximum. The rate is $m\gamma$ at the thin limit ($m = 2.47$). If the thickness is reduced with the constant surface area, the enhanced amplitude monotonically decreases in spite of increase of enhancement. It is important to increase the surface area for the amplitude. The large surface area is of no matter for detection because the nuclear dipole interaction responsible for spin transfer is so weak that the nuclei polarized at the surface contribute to the NMR signal.

The buildup rate by optical pumping was nearly an order of magnitude larger than the recovery rate of bulk chloride (Fig. 6) and twice for hydrides (Fig. 5). Therefore, we expect the thickness less than the spin diffusion length. If the thickness is 10 nm ($\xi_d \sim 0.1$), most of nuclei belong to *surface*. In addition to the crystal structure, D and γ should also change. The rate γ increases due to the quadrupole relaxation in a low symmetry crystal and the paramagnetic sites created in the film.

The film model also provides the decay rate of enhanced signal in the dark shown in Fig. 9. When the spin polarization is maximized by the continuous pumping, the injected current equilibrates with the homogeneous relaxation and the leak to substrate. Once the laser is turned off, the polarization decays through both loss channels. Therefore, the decay rate of enhanced signal is same as spin buildup rate by optical pumping.

[1] J. Ball, Nucl. Instrum. Methods A **526**, 7 (2004).
[2] T. G. Walker and W. Happer, Rev. Mod. Phys. **69**, 629 (1997).
[3] K. Ishikawa, B. Patton, Y.-Y. Jau, and W. Happer, Phys. Rev. Lett. **98**, 183004 (2007).
[4] K. Ishikawa, B. Patton, B. A. Olsen, Y.-Y. Jau, and W. Happer, Phys. Rev. A **83**, 063410 (2011).
[5] K. Ishikawa, Phys. Rev. A **84**, 013403 (2011).
[6] A. Abragam, *Principles of Nuclear Magnetism* (Oxford University Press, Oxford, UK, 1961).
[7] T. B. Reed, *Free Energy of Formation of Binary Compounds* (MIT Press, Boston, 1971).
[8] N. D. Bhaskar, J. Camparo, M. Ligare, and W. Happer, Phys. Rev. Lett. **46**, 1387 (1981).
[9] F. F. Gubaidullin, A. N. Gil'manov, V. L. Ermakov, and G. I. Pilipenko, Fiz. Tverd. Tela (Leningrad) **22**, 1890 (1980) [Sov. Phys. Solid State **22**, 1104 (1980)].
[10] A. Borgschulte, F. Pendolino, R. Gremaud, and A. Züttel, Appl. Phys. Lett. **94**, 111907 (2009).
[11] W. M. Yen and R. E. Norberg, Phys. Rev. **131**, 269 (1963).
[12] N. N. Kuzma, B. Patton, K. Raman, and W. Happer, Phys. Rev. Lett. **88**, 147602 (2002).